AMERICAN SOCIETY FOR MICROBIOLOGY | mBio®

RESEARCH ARTICLE

Candidalysins Are a New Family of Cytolytic Fungal Peptide Toxins

Jonathan P. Richardson,[a] Rhys Brown,[a] Nessim Kichik,[a] Sejeong Lee,[a] Emily Priest,[a] Selene Mogavero,[b] Corinne Maufrais,[c,d] Don N. Wickramasinghe,[a] Antzela Tsavou,[a] Natalia K. Kotowicz,[a] Olivia W. Hepworth,[a] Ana Gallego-Cortés,[a*] Nicole O. Ponde,[a§] Jemima Ho,[a] David L. Moyes,[a] Duncan Wilson,[e] Christophe D'Enfert,[d] Bernhard Hube,[b,f] Julian R. Naglik[a]

[a]Centre for Host-Microbiome Interactions, Faculty of Dentistry, Oral and Craniofacial Sciences, King's College London, London, United Kingdom
[b]Department of Microbial Pathogenicity Mechanisms, Leibniz Institute for Natural Product Research and Infection Biology, Hans Knoell Institute, Jena, Germany
[c]Institut Pasteur, Université de Paris, Bioinformatics and Biostatistics Hub, Paris, France
[d]Institut Pasteur, Université de Paris, INRAE, USC2019, Unité Biologie et Pathogénicité Fongiques, Paris, France
[e]Medical Research Council Centre for Medical Mycology at the University of Exeter, Exeter, United Kingdom
[f]Institute of Microbiology, Friedrich Schiller University, Jena, Germany

Jonathan P. Richardson and Rhys Brown contributed equally to this work. Author order was determined based on contribution to manuscript writing.

ABSTRACT Candidalysin is the first cytolytic peptide toxin identified in any human fungal pathogen. Candidalysin is secreted by *Candida albicans* and is critical for driving infection and host immune responses in several model systems. However, *Candida* infections are also caused by non-*C. albicans* species. Here, we identify and characterize orthologs of *C. albicans* candidalysin in *C. dubliniensis* and *C. tropicalis*. The candidalysins have different amino acid sequences, are amphipathic, and adopt a predominantly α-helical secondary structure in solution. Comparative functional analysis demonstrates that each candidalysin causes epithelial damage and calcium influx and activates intracellular signaling pathways and cytokine secretion. Importantly, *C. dubliniensis* and *C. tropicalis* candidalysins have higher damaging and activation potential than *C. albicans* candidalysin and exhibit more rapid membrane binding and disruption, although both fungal species cause less damage to epithelial cells than *C. albicans*. This study identifies the first family of peptide cytolysins in human-pathogenic fungi.

IMPORTANCE Pathogenic fungi kill an estimated 1.5 million people every year. Recently, we discovered that the fungal pathogen *Candida albicans* secretes a peptide toxin called candidalysin during mucosal infection. Candidalysin causes damage to host cells, a process that supports disease progression. However, fungal infections are also caused by *Candida* species other than *C. albicans*. In this work, we identify and characterize two additional candidalysin toxins present in the related fungal pathogens *C. dubliniensis* and *C. tropicalis*. While the three candidalysins have different amino acid sequences, all three toxins are α-helical and amphipathic. Notably, the candidalysins from *C. dubliniensis* and *C. tropicalis* are more potent at inducing cell damage, calcium influx, mitogen-activated protein kinase signaling, and cytokine responses than *C. albicans* candidalysin, with the *C. dubliniensis* candidalysin having the most rapid membrane binding kinetics. These observations identify the candidalysins as the first family of peptide toxins in human-pathogenic fungi.

KEYWORDS *Candida*, candidalysin, fungus, peptide toxin

Cytolytic proteins and peptide toxins are classical virulence factors of bacterial pathogens and play a major role in bacterial disease (1, 2). Human-pathogenic fungi were not known to possess such toxins until the recent discovery of candidalysin, a peptide toxin secreted by *Candida albicans* (3). *C. albicans* is normally a benign

Editor Deborah A. Hogan, Geisel School of Medicine at Dartmouth

Address correspondence to Jonathan P. Richardson, jonathan.richardson@kcl.ac.uk, or Julian R. Naglik, julian.naglik@kcl.ac.uk.

*Present address: Ana Gallego-Cortés, Department of Infectious Diseases, Vall d'Hebron University Hospital, Barcelona, Spain.

§Present address: Nicole O. Ponde, Division of Rheumatology and Clinical Immunology, University of Pittsburgh, Pittsburgh, Pennsylvania, USA.

The authors declare no conflict of interest.

Received 25 November 2021
Accepted 22 December 2021
Published 25 January 2022

member of the microbiota (4), but under certain predisposing conditions, it can cause superficial mucosal infection in healthy individuals and potentially fatal invasive and systemic infection in the immunocompromised (5).

Candidalysin is critical for *C. albicans* mucosal infections and is produced by targeted proteolytic processing of the hypha-associated protein Ece1p by kexin proteases at conserved lysine-arginine recognition sites (6, 7). Following secretion, candidalysin destabilizes the plasma membrane of epithelial cells (3, 8), triggers cellular stress resulting in necrotic cell death (9), and facilitates fungal translocation across gastrointestinal epithelial cells (10).

Host recognition of candidalysin activity comprises a critical aspect of immune defense against *C. albicans*. Candidalysin activates the epidermal growth factor receptor (EGFR) (11) and triggers innate epithelial immune responses predominantly through the mitogen-activated protein kinase (MAPK) pathway and the activating protein 1 (AP-1) transcription factor c-Fos that drives numerous cytokine responses, a process that is regulated by the MAPK phosphatase MKP1 (via the extracellular signal-regulated kinase 1 and 2 [ERK1/2] MAPK pathway) (3, 12, 13). Epithelial recognition of candidalysin activity subsequently drives a number of critically important innate cellular immune responses, including the proliferation of tissue-resident interleukin-17 (IL-17)-producing $CD4^+$ T cell receptor $\alpha\beta$-positive ($TCR\alpha\beta^+$) type 17 immune cells in murine oral tissue (14), neutrophil recruitment to the kidney (15) and brain (16) during murine systemic infection, and the secretion of IL-1β from macrophages via NLRP3 inflammasome activation (17, 18). Candidalysin also elicits protective allergic responses via platelet-mediated T helper 2 (Th2) and Th17 cell polarization (19).

Although *C. albicans* is associated with the majority of mucosal *Candida* infections, candidiasis is also caused by several non-*C. albicans* species, including *C. dubliniensis* and *C. tropicalis*, which induce varied epithelial responses *in vitro* and *in vivo* (20–24). While *C. albicans*, *C. dubliniensis*, and *C. tropicalis* exhibit differences in their abilities to maintain hyphae on epithelial cells, all three species cause epithelial damage (although to different extents) and stimulate the release of the damage-associated cytokine IL-1α (23, 25–27). Orthologs of *C. albicans ECE1* have been identified in *C. dubliniensis* and *C. tropicalis*, which exhibit differences in gene expression *in vitro* and *in vivo* in the context of vaginal immunopathology (24). However, it is unknown whether the *ECE1* genes of *C. dubliniensis* and *C. tropicalis* encode candidalysin toxins and whether these are biologically functional.

Here, we characterize the biological function of the candidalysin toxins from *C. dubliniensis* and *C. tropicalis*. Investigations with oral epithelial cells and artificial lipid membranes demonstrate that the *C. dubliniensis* and *C. tropicalis* candidalysins possess more potent cytolytic and immunostimulatory activity than *C. albicans* candidalysin despite the paradox that *C. dubliniensis* and *C. tropicalis* are considered less "pathogenic" than *C. albicans*.

This work identifies the candidalysins as a novel family of fungal peptide toxins that are functionally conserved but differ in potency.

RESULTS

Identification of candidalysin toxins in *C. dubliniensis* and *C. tropicalis*. To identify candidalysin toxins in pathogenic non-*C. albicans* species of *Candida*, we used the amino acid sequence of *C. albicans* SC5314 Ece1p to screen the PhylomeDB v4 database (28) and performed a BLASTp search at the National Center for Biotechnology Information (NCBI) for Ece1p orthologs. The screen identified Ece1p orthologs in the closely related fungal pathogens *C. dubliniensis* and *C. tropicalis*. Clustal Omega multiple-sequence alignment (29) of *C. albicans* Ece1p and the Ece1p sequences of *C. dubliniensis* and *C. tropicalis* (Fig. 1A) revealed the presence of a candidalysin-like region (designated *C. dubliniensis* $Ece1p_{59–89}$ and *C. tropicalis* $Ece1p_{68–98}$) flanked by lysine-arginine kexin recognition sites, similar to *C. albicans* candidalysin ($Ece1p_{62–92}$) (Fig. 1B). Analysis of each candidalysin-like sequence using the JPred 4 protein secondary structure

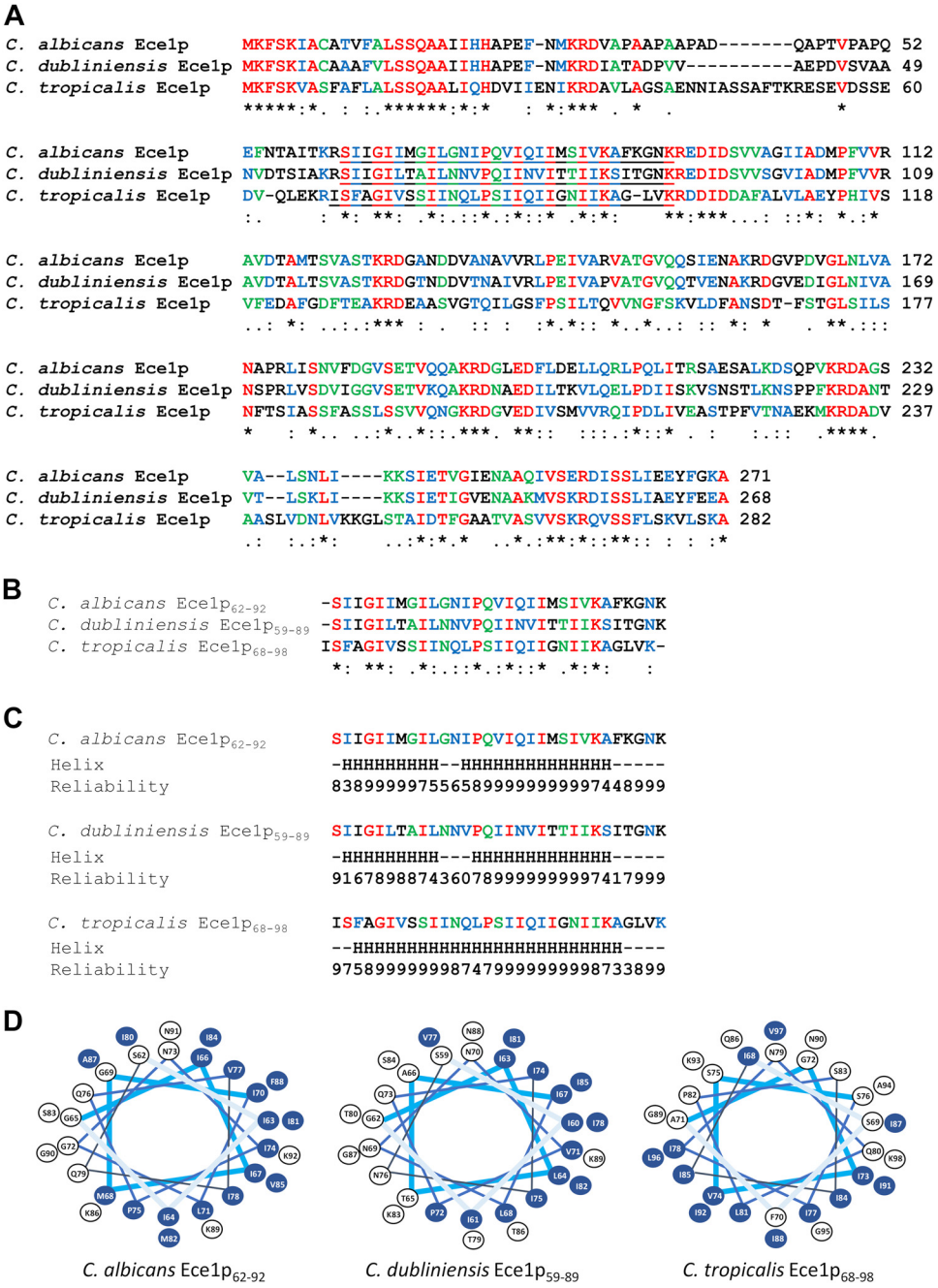

FIG 1 Identification of a candidalysin toxin in *Candida dubliniensis* and *Candida tropicalis*. (A) Clustal Omega multiple-sequence alignment of Ece1p from *C. albicans*, *C. dubliniensis*, and *C. tropicalis*. Asterisk (*), conserved residues (red); colon (:), residues with strongly similar properties (blue); period (.), residues with weakly similar properties (green). Regions corresponding to candidalysin-like peptides are underlined. (B) Clustal Omega multiple-sequence alignment of candidalysin peptides from *C. albicans*, *C. dubliniensis*, and *C. tropicalis*. (C) JPred secondary structure analysis of candidalysin peptides from *C. albicans*, *C. dubliniensis*, and *C. tropicalis*. Regions predicted to form an α-helix are identified ("H"). The reliability of prediction is scored numerically (0 to 9), where 0 is the weakest and 9 is the strongest. (D) Helical-wheel renderings of candidalysin sequences from *C. albicans*, *C. dubliniensis*, and *C. tropicalis*. Hydrophobic amino acid residues are highlighted in blue.

prediction server (30) indicated the presence of two distinct α-helix-forming regions in the peptides of *C. albicans* and *C. dubliniensis* but only a single α-helix-forming region in the peptide of *C. tropicalis* (Fig. 1C).

Helical-wheel renderings (31) of *C. dubliniensis* Ece1p$_{59–89}$ and *C. tropicalis* Ece1p$_{68–98}$ revealed an asymmetric distribution of hydrophobic amino acids similar to that of *C.*

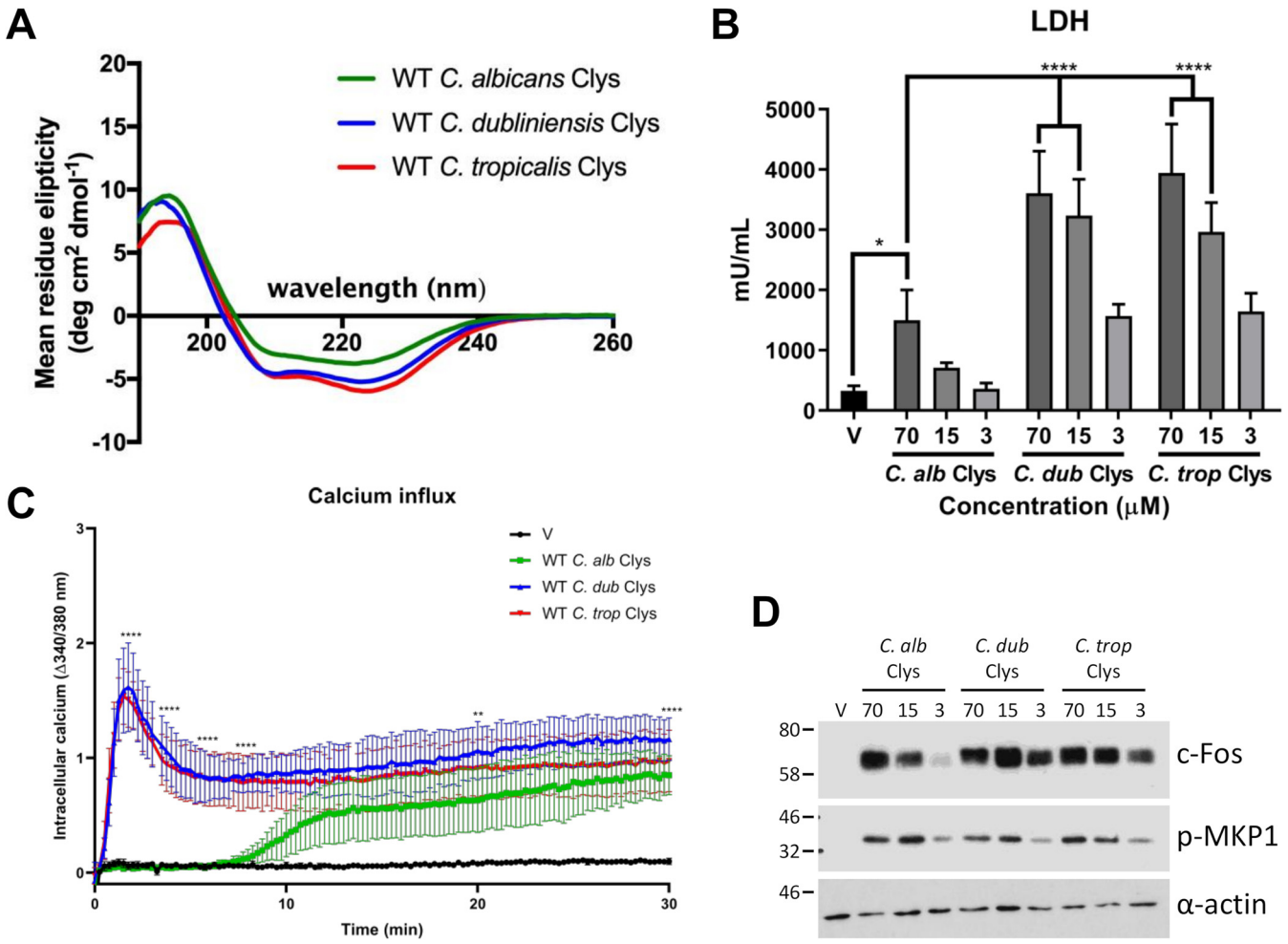

FIG 2 The candidalysin family of cytolysins exhibits different potencies on TR146 oral epithelial cells. (A) Circular dichroism spectroscopy of candidalysin (Clys) toxins from *C. albicans*, *C. dubliniensis*, and *C. tropicalis*. (B) TR146 oral epithelial cells were treated with candidalysins (70, 15, and 3 μM) from *C. albicans*, *C. dubliniensis*, and *C. tropicalis* for 24 h, and levels of cell damage were assessed by an LDH assay. Statistics are applied relative to 70 μM *C. albicans* candidalysin. For *C. albicans* candidalysin (3 μM) versus *C. dubliniensis* (3 μM) and *C. tropicalis* (3 μM) candidalysins, the *P* values were 0.0016 (**) and 0.0006 (***), respectively (n = 6 biological repeats). (C) Calcium influx in epithelial cells treated with the candidalysins (70 μM) of *C. albicans*, *C. dubliniensis*, and *C. tropicalis* for 30 min. Statistics are applied relative to WT *C. albicans* candidalysin (2, 4, 6, and 8 min) and vehicle-treated (V) cells (20 and 30 min) (n = 3 biological repeats). (D) Western blot analysis of epithelial cells treated with the candidalysins (70, 15, and 3 μM) of *C. albicans*, *C. dubliniensis*, and *C. tropicalis* for 2 h. Epithelial cell lysates (5 μg total protein) were probed with anti-c-Fos and anti-p-MKP1 antibodies. One representative blot is presented (from 3 biological repeats). Statistics are applied relative to vehicle-treated cells (n = 3 biological repeats). For panels B and C, data are presented as means and standard deviations (SD). Statistical significance was calculated using one-way ANOVA with Tukey's *post hoc* comparison test. ****, $P \leq 0.0001$; **, $P \leq 0.01$; *, $P \leq 0.05$.

albicans candidalysin (Ece1p$_{62–92}$) (Fig. 1D). Analysis of each sequence using the TANGO algorithm (32) suggested that the peptides of *C. albicans* and *C. dubliniensis*, but not that of *C. tropicalis*, were similar in their predicted abilities to form helical aggregates (see Fig. S1A in the supplemental material). Together, these data indicate that candidalysin-like toxin sequences exist in *C. dubliniensis* and *C. tropicalis* (termed candidalysins herein).

***C. dubliniensis* and *C. tropicalis* candidalysins are α-helical cytolysins that exhibit potent damage-inducing ability.** To investigate the biological activity of these newly discovered candidalysins, peptides corresponding to *C. dubliniensis* Ece1p$_{59–89}$ (SIIGILTAILNNVPQIINVITTIIKSITGNK) and *C. tropicalis* Ece1p$_{68–98}$ (ISFAGIVSSIIN QLPSIIQIIGNIIKAGLVK) were synthesized, and their biophysical and biological properties were compared to those of *C. albicans* candidalysin (SIIGIIMGILGNIPQVIQIIMSIVKA FKGNK). Circular dichroism (CD) spectroscopy analysis revealed that the *C. dubliniensis* and *C. tropicalis* candidalysins adopt a predominantly α-helical secondary structure in solution, similarly to *C. albicans* candidalysin (Fig. 2A).

C. albicans candidalysin causes epithelial damage, which can be measured by the release of lactate dehydrogenase (LDH) (3, 8, 10). Therefore, we assessed the ability of each newly discovered candidalysin to cause epithelial damage by treating TR146 oral epithelial cells with the three candidalysins (70, 15, and 3 μM, representing highly lytic, moderately lytic, and sublytic concentrations of *C. albicans* candidalysin) for 24 h and quantified LDH activity. As expected, the *C. albicans* candidalysin caused significant damage in a dose-dependent manner. Surprisingly, while *C. dubliniensis* and *C. tropicalis* fungi cause less damage to epithelial cells than *C. albicans* (23), the candidalysins of *C. dubliniensis* and *C. tropicalis* caused significantly greater damage at all concentrations than *C. albicans* candidalysin (Fig. 2B).

C. albicans candidalysin causes calcium influx into epithelial cells (3). Accordingly, we investigated the ability of *C. dubliniensis* and *C. tropicalis* candidalysins to induce calcium influx in oral epithelial cells. All three candidalysins induced a significant level of calcium influx between 30 and 180 min (Fig. S1B). However, *C. dubliniensis* and *C. tropicalis* candidalysins induced significantly more rapid calcium influx than *C. albicans* candidalysin within the first 10 min (Fig. 2C). These data demonstrate that the *C. dubliniensis* and *C. tropicalis* candidalysins are α-helical peptide toxins that are more potent in their ability to cause epithelial damage and calcium influx than *C. albicans* candidalysin.

***C. dubliniensis* and *C. tropicalis* candidalysins potently activate epithelial immune responses.** *C. albicans* candidalysin activates epithelial cells via the MAPK pathway comprising c-Fos and MKP1 signaling (3, 8, 12, 13, 33). To determine whether the *C. dubliniensis* and *C. tropicalis* candidalysins induce similar responses, oral epithelial cells were treated with all three candidalysins (70, 15, and 3 μM) for 2 h, and c-Fos expression/MKP1 phosphorylation was assessed by Western blotting. All candidalysins activated epithelial c-Fos/p-MKP1 signaling in a dose-dependent manner; however, *C. dubliniensis* and *C. tropicalis* candidalysins upregulated c-Fos more potently at lower concentrations than *C. albicans* candidalysin (Fig. 2D).

Epithelial responses to *C. albicans* candidalysin culminate in the secretion of cytokines and chemokines required for the coordination of appropriate innate immune responses (3, 8, 12–14, 33). Therefore, we treated oral epithelial cells with all three candidalysins (70, 15, and 3 μM) for 24 h and quantified the secretion of interleukin-1α (IL-1α), IL-1β, IL-6, granulocyte colony-stimulating factor (G-CSF), and granulocyte-macrophage colony-stimulating factor (GM-CSF). All three candidalysins induced these cytokines in a dose-dependent manner; however, in keeping with our above-described findings, the *C. dubliniensis* and *C. tropicalis* candidalysins were more potent than *C. albicans* candidalysin at inducing IL-1α, IL-1β, and IL-6 at lower concentrations (15 and 3 μM) (Fig. 3A to E). *C. dubliniensis* candidalysin (15 μM) stimulated significantly more IL-1α secretion than did *C. albicans* candidalysin. *C. dubliniensis* and *C. tropicalis* candidalysins (15 μM) induced significantly more secretion of IL-1β, while *C. tropicalis* candidalysin (3 μM) induced significantly more secretion of IL-1β than with the same concentration of *C. albicans* candidalysin. Similar concentrations of G-CSF and GM-CSF were secreted in response to all three candidalysins, except for *C. dubliniensis* candidalysin at 70 μM, which failed to induce these two cytokines (Fig. 3D and E), presumably through excess toxicity. Collectively, these data demonstrate that the *C. dubliniensis* and *C. tropicalis* candidalysins are potent inducers of epithelial immune signaling mechanisms.

***C. dubliniensis* and *C. tropicalis* candidalysins exhibit rapid real-time permeabilization of artificial lipid bilayers.** To further investigate the observed difference in candidalysin potencies, we used Orbit 16 technology to quantify the real-time binding of all three candidalysins to artificial 1,2-diphytanoyl-*sn*-glycero-3-phosphocholine (DPhPC) planar lipid bilayers. Candidalysins (2, 4, 6, 8, and 10 μM) from *C. albicans*, *C. dubliniensis*, and *C. tropicalis* were applied to DPhPC planar lipid bilayers, and the dwell time (defined as the time that elapsed between candidalysin addition and bilayer permeabilization) was quantified (Fig. S1C). The candidalysins of *C. dubliniensis* and *C. tropicalis* were far more rapid (by a factor of 4 to 7) at permeabilizing a

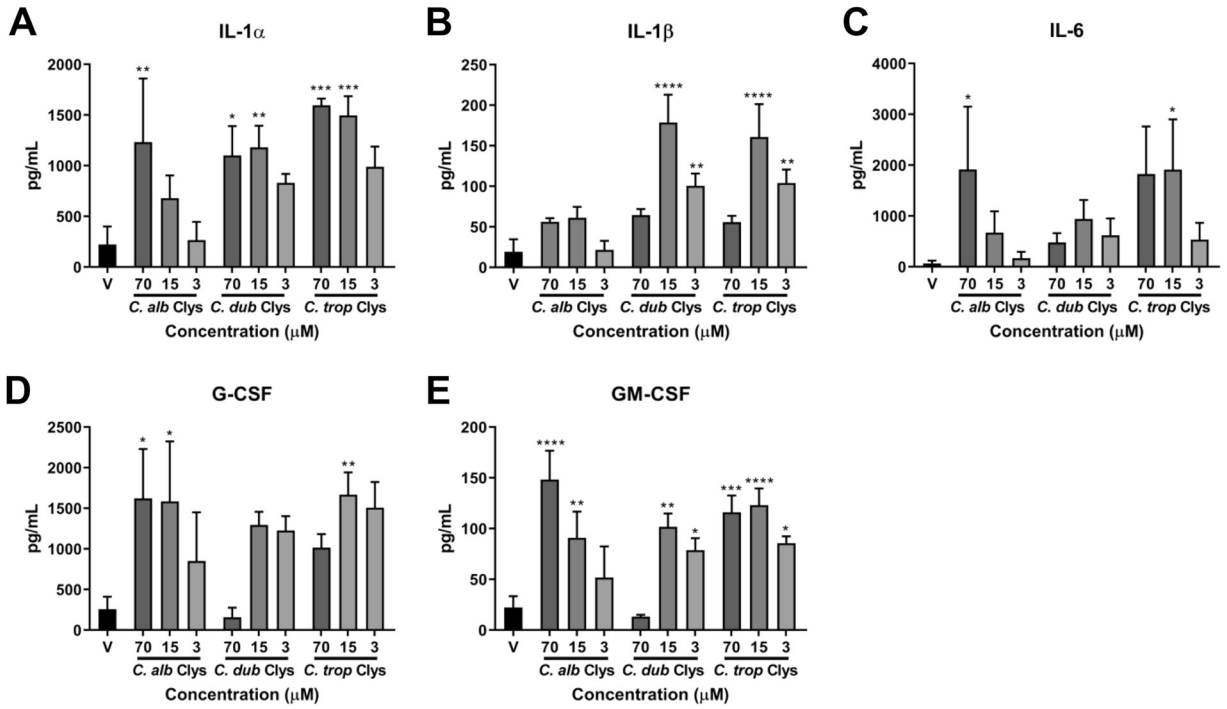

FIG 3 The candidalysins induce different levels of cytokine secretion. Quantification of cytokines (IL-1α, IL-1β, IL-6, G-CSF, and GM-CSF) secreted from epithelial cells treated with the candidalysins (70, 15, and 3 μM) of *C. albicans*, *C. dubliniensis*, and *C. tropicalis* is shown. Statistics are applied relative to vehicle-treated cells. Data are presented as means and SD from 3 biological repeats. For IL-1α, for *C. dubliniensis* candidalysin (15 μM) versus *C. albicans* candidalysin (15 μM), the *P* value was 0.0360 (*). For IL-1β, for *C. dubliniensis* and *C. tropicalis* candidalysins (15 μM) versus *C. albicans* candidalysin (15 μM), the *P* values were $<$0.0001 (****) and 0.0002 (***), respectively. For IL-1β, for *C. tropicalis* candidalysin (3 μM) versus *C. albicans* candidalysin (3 μM), the *P* value was 0.0021 (**). Statistical significance was calculated using one-way ANOVA with Tukey's *post hoc* comparison test. ****, $P \leq 0.0001$; ***, $P \leq 0.001$; **, $P \leq 0.01$; *, $P \leq 0.05$.

DPhPC bilayer than *C. albicans* candidalysin at a concentration of 2 μM (compare representative traces in Fig. 4A to C and averaged data in Fig. 4D). Collectively, these data demonstrate that candidalysins from *C. dubliniensis* and *C. tropicalis* permeabilize DPhPC membranes more rapidly than *C. albicans* candidalysin.

***C. albicans*, *C. dubliniensis*, and *C. tropicalis* exhibit differences in *ECE1* gene expression.** Hyphal growth and maintenance are known to differ among *C. albicans*, *C. dubliniensis*, and *C. tropicalis* and between strains of each species (23, 25, 27). Since the expression of *C. albicans ECE1* (encoding candidalysin) is strongly induced during interactions with epithelial cells, we investigated the levels of *ECE1* gene expression between species during infection of oral epithelial cells. Oral epithelial cells were infected with *C. albicans*, *C. dubliniensis*, and *C. tropicalis* for 24 h, and *ECE1* gene expression was analyzed by reverse transcription-quantitative PCR (RT-qPCR). As expected, *C. albicans* expressed significant levels of *ECE1* (11,000-fold) in the presence of epithelial cells compared to the preculture. In contrast, no difference in *ECE1* gene expression was observed in *C. dubliniensis* or *C. tropicalis* in the presence of epithelial cells compared to the preculture (Fig. 4E). These data suggest that while the *C. dubliniensis* and *C. tropicalis* synthetic candidalysins are more potent than the *C. albicans* toxin when applied to oral epithelial cells, neither native candidalysin appears to be produced by representative strains of each species during infection of oral epithelial cells *in vitro*.

Ectopic expression of *C. dubliniensis* and *C. tropicalis ECE1* in *C. albicans*. A direct comparison of *C. albicans*, *C. dubliniensis*, and *C. tropicalis* pathogenicities is severely hampered by differences in hypha formation and elongation and *ECE1* gene expression. To mitigate these issues, we used CIp10 (34) to create plasmids where the *ECE1* genes of *C. dubliniensis* and *C. tropicalis* were placed under the control of the *C. albicans* SC5314 *ECE1* promoter. These constructs were introduced into a *C. albicans*

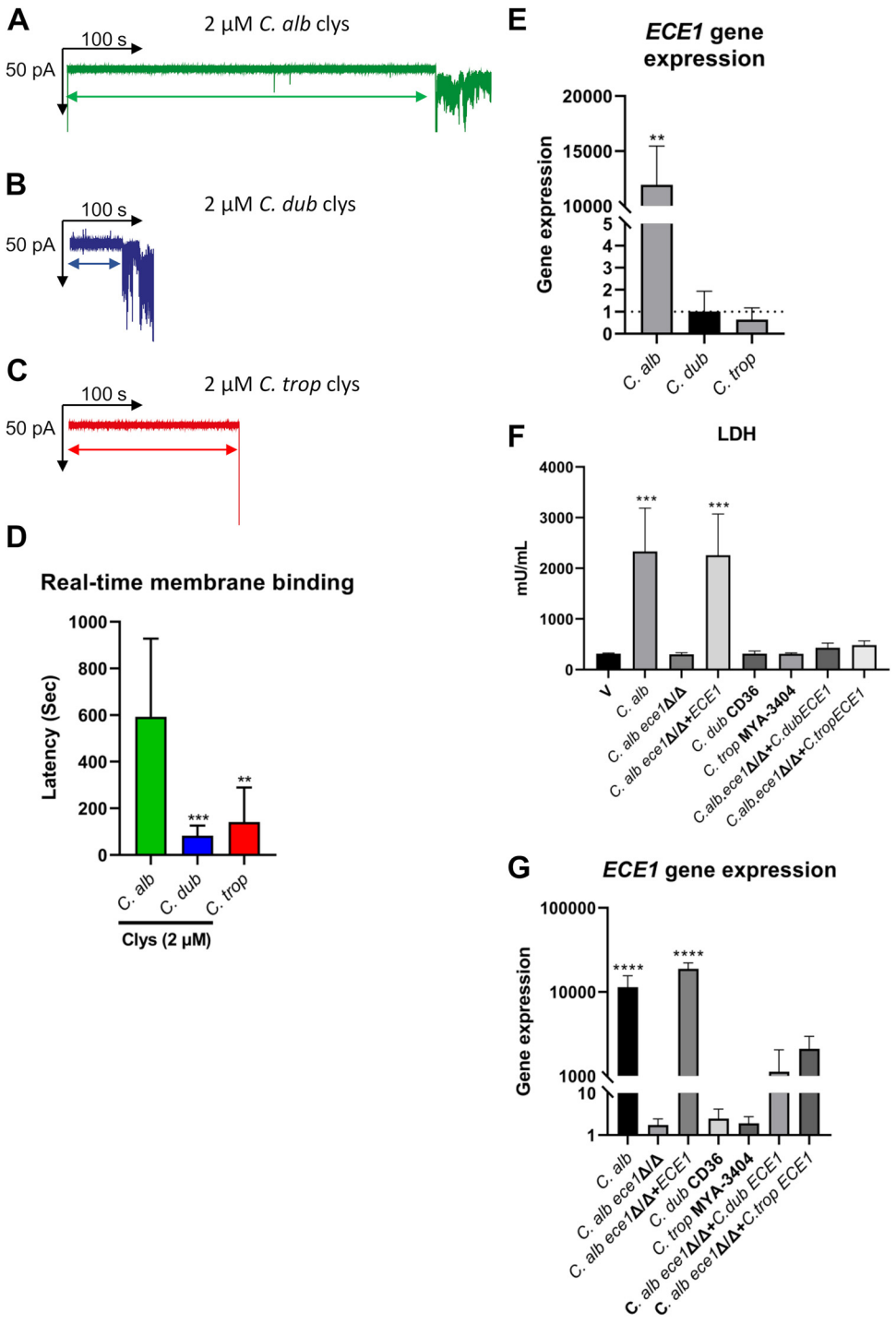

FIG 4 Candidalysins exhibit differences in real-time membrane permeabilization, and *C. albicans*, *C. dubliniensis*, and *C. tropicalis* fungi exhibit differences in *ECE1* gene expression. (A to C) Individual representative traces quantifying the dwell time (defined as the time that elapsed between candidalysin addition and bilayer permeabilization) for *C. albicans* (A), *C. dubliniensis* (B), and *C. tropicalis* (C) candidalysins at 2 μM. (D) Comparison of average dwell times for 2 μM candidalysins from *C. albicans*, *C. dubliniensis*, and *C. tropicalis*. Data are presented as means and SD from 10 biological repeats. Statistical significance was calculated using a two-tailed unpaired *t* test (versus *C. albicans* candidalysin). ***, $P \leq 0.001$; **, $P \leq 0.01$. (E) *ECE1* gene expression in *C. albicans*, *C. dubliniensis*, and *C. tropicalis* was quantified in the presence of epithelial cells by RT-qPCR after 24 h. Gene expression is presented relative to the 0-h samples cultured in YPD medium at 30°C in the absence of epithelial cells (dotted line). The fold change ($2^{\Delta\Delta CT}$) was calculated for each strain using the threshold cycle method in comparison to *ACT1* as the reference gene. Data are the means and SD from 3 biological replicates. Statistical significance was calculated using a two-tailed unpaired *t* test (versus the time zero control). **, $P \leq 0.01$. (F) TR146 oral epithelial cells were infected with *C. albicans* expressing *C. dubliniensis ECE1* (*C.alb.ece1*Δ/Δ+*C.dubECE1*) and

(Continued on next page)

*ece1*Δ/Δ null mutant (3) to enable comparisons of candidalysin activities without differences in hyphal growth and maintenance and gene expression. The integration of each construct into the *C. albicans* genome was verified by PCR analysis of genomic DNA (gDNA). All transformants were viable and displayed similar levels of filamentation when cultured on epithelial cells.

We infected oral epithelial cells with *C. albicans* harboring the *ECE1* gene of *C. dubliniensis* (*C.alb.ece1*Δ/Δ+*C.dubECE1*) or *C. tropicalis* (*C.alb.ece1*Δ/Δ+*C.tropECE1*) and assessed epithelial damage after 24 h by an LDH assay. *C. albicans ece1*Δ/Δ null and *ece1*Δ/Δ+*ECE1*, *C. dubliniensis* CD36, and *C. tropicalis* MYA-3404 were used as controls. All control species and strains behaved as expected, with *C. albicans* inducing cell damage in an *ECE1*-dependent manner (3) and *C. dubliniensis* and *C. tropicalis* exhibiting minimal levels of damage compared with *C. albicans*, as observed previously (23). Notably, only minimal levels of epithelial damage were caused by *C.alb.ece1*Δ/Δ+*C.dubECE1* and *C.alb.ece1*Δ/Δ+*C.tropECE1* (Fig. 4F). To determine if *ECE1* gene expression was impaired in these ectopic mutants, we infected epithelial cells with *C.alb.ece1*Δ/Δ+*C.dubECE1* and *C.alb.ece1*Δ/Δ+*C.tropECE1* for 24 h and quantified gene expression by RT-qPCR. As expected, the *C. albicans* parent strain and the *C. albicans ece1*Δ/Δ+*ECE1* mutant expressed significant levels of *ECE1* in the presence of epithelial cells, while wild-type (WT) *C. dubliniensis* CD36 and *C. tropicalis* MYA-3404 did not express *ECE1*. Surprisingly, while the *C.alb.ece1*Δ/Δ+*C.dubECE1* and *C.alb.ece1*Δ/Δ+*C.tropECE1* ectopic mutants also expressed *ECE1*, expression was much reduced compared with that of the *C. albicans ece1*Δ/Δ+*ECE1* control (Fig. 4G). These data demonstrate that the ectopic expression of *C. dubliniensis* and *C. tropicalis ECE1* in *C. albicans* fails to induce significant epithelial damage.

DISCUSSION

Numerous pore-forming toxins are found in nature, including colicins, cytolysins, hemolysins, aerolysins, and cholesterol-dependent cytolysins of bacterial pathogens (reviewed in references 1 and 2); actinoporins of sea anemones (35); fungal killer toxins (36); and antimicrobial peptides (37). In 2016, we discovered candidalysin, the first cytolytic peptide toxin identified in a human fungal pathogen. Candidalysin is secreted by *C. albicans* and is critical for disease pathology during mucosal and systemic infections, the facilitation of fungal translocation across intestinal epithelial cells, and the amplification of immune responses (3, 8, 10, 14–16).

Although differences in the levels of *ECE1* gene expression between *Candida* species have been reported during vaginal infection *in vitro* and *in vivo* (24), it was unknown whether the *C. dubliniensis* and *C. tropicalis ECE1* genes also encode candidalysin peptide toxins and whether these are functional. We now identify the candidalysins as a new family of functionally active peptide toxins and the first family of peptide cytolysins in human-pathogenic fungi.

Ece1p and candidalysin orthologs were found in *C. dubliniensis* and *C. tropicalis*, which are pathogenic to humans and capable of forming hyphal filaments when cultured in the presence of epithelial cells (23). Notably, other pathogenic *Candida* species, including *C. glabrata*, *C. parapsilosis*, and the emerging pathogen *C. auris*, do not harbor Ece1p or candidalysin orthologs, which suggests that the damage potential and pathogenicity of these species are dependent on other fungal factors.

FIG 4 Legend (Continued)

C. tropicalis ECE1 (*C.alb.ece1*Δ/Δ+*C.tropECE1*) for 24 h, and levels of cell damage were assessed by an LDH assay. Statistics are applied relative to vehicle-treated cells. Data are the means and SD from 3 biological repeats. (G) *ECE1* gene expression in the *C.alb.ece1*Δ/Δ+*C.dubECE1* and *C.alb.ece1*Δ/Δ+*C.tropECE1* mutants was quantified in the presence of epithelial cells by RT-qPCR after 24 h. Gene expression is presented relative to the 0-h samples cultured in YPD medium at 30°C in the absence of epithelial cells. The fold change ($2^{\Delta\Delta CT}$) was calculated for each strain using the threshold cycle method in comparison to *ACT1* as the reference gene. Data are the means and SD from 3 biological replicates. Statistical significance in panels F and G was calculated using one-way ANOVA with Tukey's *post hoc* comparison test. ****, $P \leq 0.0001$; ***, $P \leq 0.001$.

TABLE 1 Physical properties and epithelial responses to candidalysins

Property	Strength of response to candidalysin from[a]:		
	C. albicans	*C. dubliniensis*	*C. tropicalis*
Amphipathicity	+++++	+++++	++++
α-Helicity	+++	++++	++++
Cellular damage	+++	+++++	+++++
Calcium influx	+++	+++++	+++++
MAPK signaling	+++	+++++	+++++
Cytokine secretion	+++	+++++	+++++
Membrane permeabilization	+++	+++++	++++

[a]+++, comparatively low potency; ++++, comparatively moderate potency; +++++, comparatively high potency.

The candidalysins of *C. albicans*, *C. dubliniensis*, and *C. tropicalis* exhibit clear differences in potency. This was evidenced by (i) the greater LDH activity, more rapid calcium influx, and stronger c-Fos responses induced by the *C. dubliniensis* and *C. tropicalis* candidalysins than those induced by the *C. albicans* candidalysin; (ii) the greater release of the damage-associated cytokine IL-1α by the *C. dubliniensis* and *C. tropicalis* candidalysins but not the *C. albicans* candidalysin at lower concentrations (15 and 3 μM); and (iii) the significantly shorter time for *C. dubliniensis* and *C. tropicalis* candidalysins (2 μM) to permeabilize artificial DPhPC planar lipid bilayers than for *C. albicans* candidalysin (summarized in Table 1). The greater potency of *C. dubliniensis* and *C. tropicalis* candidalysins is an intrinsic property of their respective amino acid sequences since the DPhPC planar lipid bilayers used in the permeability assays did not contain heterologous protein (i.e., purified receptors).

Interestingly, while the *C. dubliniensis* and *C. tropicalis* candidalysins have more damaging and activating potential than *C. albicans* candidalysin, *C. dubliniensis* and *C. tropicalis* fungi are "less pathogenic" than *C. albicans*. This discrepancy in pathogenicity likely corresponds to the expression level and context of candidalysin processing, secretion, and delivery to the host membrane. We previously noted that in the presence of epithelial cells, hypha formation and maintenance in *C. dubliniensis* and *C. tropicalis* are poor compared to those in *C. albicans* SC5314 (23). Assuming that *ECE1* gene expression is associated with hypha formation in *C. dubliniensis* and *C. tropicalis*, similarly to *C. albicans*, it would be expected that *ECE1* expression (and, hence, candidalysin production) will also be far lower in these species. Indeed, clear differences in the levels of *ECE1* gene expression were observed in *C. albicans*, *C. dubliniensis*, and *C. tropicalis* when cultured in the presence of oral epithelial cells. Furthermore, similar analyses demonstrate that *C. dubliniensis* and *C. tropicalis* express far less *ECE1* than *C. albicans* when cultured on vaginal epithelial cells *in vitro*, and no *ECE1* expression was observed *in vivo* in a murine vaginitis infection model (24). Thus, the apparent disparity between the candidalysin potency and fungal pathogenicity of these three *Candida* species can be explained by differences in hypha formation, hypha maintenance, and levels of *ECE1* gene expression and candidalysin secretion during infection.

The *C. albicans* strain used in this study (SC5314) is more pathogenic and induces stronger damage than other clinical strains of *C. albicans* (38, 39). Notably, clinical *C. albicans* strains often exhibit impaired hyphal maintenance on epithelial cells compared with strain SC5314 (13, 39). Furthermore, *ECE1* gene expression in clinical strains only partially correlated with epithelial damage *in vitro*, independently of hypha formation (39). However, this discrepancy was recently clarified by a study that demonstrated that a combination of sustained hypha formation, *ECE1* expression, and candidalysin secretion into an invasion pocket was critical for sustained damage induced by invading *Candida* species during mucosal infection (40).

To mitigate differences in hypha formation and maintenance, *ECE1* gene expression, and invasion pocket formation among *C. albicans*, *C. dubliniensis*, and *C. tropicalis*, the *ECE1* genes of *C. dubliniensis* and *C. tropicalis* were placed under the control of the *C. albicans*

ECE1 promoter and introduced into a *C. albicans ece1*Δ/Δ mutant. The inability of the *C.alb.ece1*Δ/Δ+*C.dubECE1* and *C.alb.ece1*Δ/Δ+*C.tropECE1* ectopic mutants to cause epithelial damage was unexpected, but this was likely due to reduced *ECE1* gene expression levels resulting in insufficient accumulation of candidalysin in the invasion pocket for damage to occur. These observations suggest that there are additional levels of regulation of *ECE1* gene expression or transcript stability that prevent the creation of a strain that expresses similar levels of *ECE1* transcripts encoding candidalysins from different species.

The question remains as to the biological significance of a more potent toxin in a less pathogenic *Candida* species. One possibility is that these toxins are actively suppressed, via either reduced hypha formation or specific *ECE1* gene targeting, to prevent excess toxicity and immune induction. Another possibility is that the niches where the candidalysins of *C. dubliniensis* and *C. tropicalis* are strongly expressed for the benefit of the fungus have not yet been identified. Such questions can be addressed in future investigations.

In summary, this work identifies the candidalysins as a new family of fungal peptide toxins, which have similar properties but differing potencies.

MATERIALS AND METHODS

Candidalysin peptides. The candidalysin peptides used in this study have the following amino acid sequences: SIIGIIMGILGNIPQVIQIIMSIVKAFKGNK for *C. albicans* candidalysin, SIIGILTAILNNVPQIINVITTIIKSITGNK for *C. dubliniensis* candidalysin, and ISFAGIVSSIINQLPSIIQIIGNIIKAGLVK for *C. tropicalis* candidalysin. All peptides were purchased from Peptide Protein Research Ltd. (UK). Each peptide was synthesized using standard 9-fluorenylmethoxy carbonyl (Fmoc) chemistry and purified by high-performance liquid chromatography (HPLC) to a minimum purity of 95%. Peptide purity and experimental molecular mass were further verified by liquid chromatography-tandem mass spectrometry (LC-MS/MS).

Antibodies. p-DUSP1/MKP1 (S359) and c-Fos rabbit monoclonal antibodies were purchased from Cell Signaling Technologies (catalog numbers 2857 and 2250, respectively). Actin (clone C4) mouse monoclonal antibody was purchased from Millipore (catalog number MAB1501). Peroxidase-conjugated AffiniPure goat anti-mouse and anti-rabbit IgG secondary antibodies were purchased from Jackson ImmunoResearch (catalog numbers 115-035-062 and 111-035-003, respectively).

Oligonucleotides. The following oligonucleotide primers (5′ to 3′) were used to quantify *ECE1* gene expression: forward (Fw) primer CTTTATCTTCTCAAGCTGC and reverse (Rev) primer CAACAACAGAATCAA TATCTTC for *C. albicans* SC5314, Fw primer GCTGATCCTGTTGTTGCTGAACC and Rev primer ATGGCATATCAGCA ATGACACCAG for *C. dubliniensis* CD36, Fw primer GATGCTGTCTTAGCTGGTTCTG and Rev primer CATCTCTCTTA ACAAGGCCAGC for *C. tropicalis* MYA-3404, and Fw primer CCAGGTATTGCTGAACGTATGC and Rev primer GGACCAGATTCGTCGTATTCTTG for universal *ACT1*. The following oligonucleotide primers (5′ to 3′) were used to verify the genomic integration of Clp10 into the *C. albicans* genome: Fw primer CGCCAAAGAGTT TCCCCTATTATC (RPF-2) and Rev primer CACAACAGAGCTTCTAAC (ECE-check1) for the 5′ integration site and Fw primer GGAGTTGGATTAGATGATAAAGGTGATGG (URA-F2) and Rev primer GAGCAGTGTACACACACACAT CTTG (RPF-1) for the 3′ integration site.

Plasmid construction. A Clp10 plasmid (34) containing an MluI/SalI insert comprising 3,128 bp of 5′ intergenic sequence, the *C. albicans ECE1* gene, and 373 bp of 3′ intergenic sequence (3) was modified to express the *ECE1* genes of *C. dubliniensis* and *C. tropicalis*. Plasmid inserts were synthesized and cloned into recipient Clp10 by GeneArt (Thermo Fisher). Briefly, the *C. albicans ECE1* gene was excised from the Clp10 plasmid described above and replaced with *C. dubliniensis ECE1* and *C. tropicalis ECE1* to yield Clp10 constructs containing *ECE1* from *C. albicans*, *C. dubliniensis*, and *C. tropicalis* with identical 5′- and 3′-flanking intergenic sequences. The sequence of each insert was verified by DNA sequencing. Constructs were linearized by digestion with StuI prior to transformation.

Transformation of *C. albicans* and extraction of genomic DNA. A uridine-auxotrophic *ece1*-null mutant [*ece1*Δ/Δ (*ura*$^-$)] was transformed with 15 μg of linearized plasmid DNA using a lithium acetate method modified from a method described previously (41). Transformants were selected on minimal (SD) agar medium and restreaked onto fresh SD agar to ensure stability, and genomic DNA was extracted using phenol-chloroform-isoamyl alcohol and glass bead lysis. The successful integration of each construct into the *C. albicans* genome (at the RPS1 locus) was confirmed by PCR amplification across the 5′ and 3′ integration sites.

Mammalian cell culture. All experiments were performed using the TR146 human oral epithelial cell line (42) purchased from the European Collection of Authenticated Cell Cultures. Cultures were verified to be mycoplasma-free by PCR. Cells were cultured in a Dulbecco modified Eagle medium (DMEM)–F-12 medium nutrient mixture (1:1) plus L-glutamine (Life Technologies) supplemented with 15% (vol/vol) heat-inactivated fetal bovine serum (Life Technologies) and 1% (vol/vol) penicillin-streptomycin (Sigma) at 37°C with 5% CO_2.

Fungal culture, infection of epithelial cells, and induction of hyphal growth. *C. albicans* SC5314, *C. dubliniensis* CD36, and *C. tropicalis* MYA-3404 were cultured in yeast extract-peptone-dextrose (YPD) liquid medium overnight at 30°C in a shaking incubator at 180 rpm. Fungi were washed twice in phosphate-buffered saline (PBS), added to epithelial cells at a multiplicity of infection (MOI) of 0.01, and incubated at 37°C with 5% CO_2 in a humidified incubator for 24 h. Induction of hyphal growth was performed in the presence of TR146 oral epithelial cells (MOI of 0.01) for 24 h.

Circular dichroism spectroscopy. Candidalysin peptides were reconstituted in sterile water (10 mg/mL stock concentration) and further diluted to 0.2 mg/mL in buffer (10 mM Tris [pH 7.0], 50 mM NaCl). Circular dichroism was performed using a Chirascan spectrometer (Applied Photophysics) at 20°C, at wavelengths of 190 to 260 nm with intervals of a 0.5 bandwidth, 2 s, and 2 repeats for each acquisition point. CD spectra were acquired using a 1-mm-path-length quartz cuvette (100-QS). All acquired spectra were averaged and corrected for background and buffer contributions, and the net spectra were smoothed with a Savitzky-Golay filter (window 3).

Treatment of epithelial cells with candidalysin peptides. Prior to infection, confluent oral epithelial cells were serum starved overnight, and all experiments were carried out in serum-free DMEM–F-12 medium. Epithelial cells were treated with candidalysin peptides at the indicated concentrations for maxima of 24 h (damage and cytokine assays), 3 h (calcium), and 2 h (Western blotting). Treated cells were cultured at 37°C with 5% CO_2.

Epithelial cell damage assay. Damage to oral epithelial cells was quantified using a Cytox 96 nonradioactive cytotoxicity assay kit (Promega) according to the manufacturer's instructions. Recombinant porcine lactate dehydrogenase (Sigma) was used to create a standard curve.

Quantification of calcium influx. Epithelial cells were seeded into opaque, clear-bottomed, 96-well plates (Greiner) at a density of 5×10^5 cells/mL; cultured to confluence overnight; and serum starved for 24 h. A solution containing 2.5 μM Fura-2 AM (Thermo Scientific) and 500 μM probenecid (Sigma) was prepared in a saline solution (140 mM NaCl, 5 mM KCl, 1 mM $MgCl_2$, 2 mM $CaCl_2$, 10 mM glucose, 10 mM HEPES [pH 7.4]). Serum-free medium was removed and replaced with 50 μL of a Fura-2 AM–probenecid-containing saline solution, and the mixture was incubated at 37°C with 5% CO_2 in the dark for 60 min. Following incubation, the Fura-2 AM–probenecid solution was removed and replaced with 50 μL of a saline solution. The plate was read on a FlexStation 3 multimode microplate reader (Molecular Devices). Samples were excited at 240/280 nm, and fluorescence was detected at 520 nm. For 30-min time course recordings (Fig. 2C), readings were taken every 15 s. For 180-min time course recordings (see Fig. S1 in the supplemental material), readings were taken every 60 s for the first 30 min and then every 5 min for 2.5 h. Results were expressed as a ratio between 340 and 380 nm.

Protein extraction from TR146 oral epithelial cells. Tissue culture plates were placed on ice, and cells were washed with 1 mL of ice-cold PBS and then lysed with 120 μL of a modified radioimmunoprecipitation assay (RIPA) buffer (50 mM Tris-HCl [pH 7.4], 150 mM NaCl, 1 mM EDTA, 1% Triton X-100, 1% sodium deoxycholate, 0.1% SDS) supplemented with 1× protease inhibitors (Thermo Scientific) and 1× phosphatase inhibitors (Sigma). A sterile cell scraper was used to detach cells from the surface of the plate. After scraping, crude cell extracts were collected, transferred to microcentrifuge tubes, and incubated on ice for 30 min. Following incubation, extracts were clarified by centrifugation in a benchtop microcentrifuge at 16,200 × *g* at 4°C for 10 min. Clarified extracts were collected, and the protein concentration was estimated using a bicinchoninic acid assay (Thermo Scientific) according to the manufacturer's instructions.

SDS-PAGE and Western blotting. Proteins were resolved by electrophoresis on 12% SDS-PAGE gels using a mini-Protean Tetra cell system (Bio-Rad). Electrophoresed proteins were transferred to a nitrocellulose membrane (Bio-Rad) using a mini-Transblot electrophoretic transfer cell (Bio-Rad). Membranes were blocked in 1× Tris-buffered saline (TBS; Severn Biotech) containing 0.001% (vol/vol) Tween 20 (Acros Organics) and 5% (wt/vol) fat-free milk powder (Sainsbury's). c-Fos, p-DUSP1/MKP1, and α-actin primary antibodies were diluted (1:3,000, 1:1,000, and 1:10,000, respectively) in TBS-Tween and 5% milk, and membranes were incubated overnight at 4°C with gentle shaking (c-Fos and p-DUSP1/MKP1) or for 1 h at room temperature with gentle shaking (α-actin). Following incubation, membranes were washed with 1× TBS containing 0.001% (vol/vol) Tween 20, diluted (1:10,000) horseradish peroxidase (HRP)-conjugated secondary antibody was added, and membranes were incubated for 1 h at room temperature. Membranes were washed as described above and exposed to the Immobilon Western chemiluminescent HRP substrate (Millipore) prior to visualization by exposure to film (GE Healthcare). α-Actin was used as a loading control.

Quantification of cytokine release from TR146 oral epithelial cells. Exhausted cell culture medium was collected, and the concentration of cytokines was determined using magnetic microparticles (R&D Systems) specific for human IL-1α, IL-1β, IL-6, G-CSF, and GM-CSF using a magnetic Luminex performance assay (Bio-Techne) and the Bio-Plex 200 system (Bio-Rad) according to the manufacturers' instructions. Data were analyzed using Bioplex Manager 6.1 software.

Quantification of bilayer permeabilization. Current measurements were performed using multiple planar lipid bilayers and an Orbit 16 system (Nanion). The horizontal bilayers were formed over 16-channel multielectrode-cavity-array (MECA) chips (Ionera) using 1,2-diphytanoyl-*sn*-glycero-3-phosphocholine (DPhPC) lipids (Avanti Polar Lipids) dissolved in octane (25 mg mL^{-1}). Both *cis* (grounded) and *trans* cavities above and below the bilayers were filled with an electrolyte solution containing 0.1 M KCl and 20 mM HEPES (pH 7.4). Candidalysin peptides dissolved in water were added to the *cis* side of bilayers at final concentrations of 2, 4, 6, 8, and 10 μM. A constant voltage of −50 mV was applied, and current changes were monitored for 10 min at room temperature. Current traces were acquired at a sampling frequency of 10 kHz using Element Data Recorder software (EDR 3.8.3). Current analysis was performed using Clampfit 10.3 (Molecular Devices). Plots were generated using GraphPad software.

RNA extraction. Epithelial cells were infected with *Candida* species for 24 h (MOI = 0.01). Exhausted culture medium was collected, and nonadherent fungi were pelleted by centrifugation. Adherent fungi were rinsed with ice-cold PBS, loosened with a cell scraper, and added to the pelleted sample. Fungi were washed with 1 mL of ice-cold PBS, resuspended in a final volume of 500 μL, added to a cryovial containing an ~1/3 volume of acid-washed glass beads (0.5 mm; Thistle Scientific), and bead beaten four times at 4.5 m/s^2 for 30 s using a FastPrep-24 system (MP Bio). The lysates were removed, and RNA was extracted using a MasterPure yeast RNA purification kit (Lucigen) according to the manufacturer's instructions. The removal of

contaminating gDNA was performed according to kit instructions. For the 0-h control samples, RNA was extracted from 500 μL of each YPD fungal culture in the absence of epithelial cells.

Quantification of *ECE1* gene expression. cDNA was synthesized using a QuantiTect reverse transcription kit (Qiagen) and 600 ng of the RNA template. cDNA samples were then used for qPCR using Hot FIREPol EvaGreen qPCR supermix (Solis BioDyne). Primers (universal forward and reverse primers for *ACT1* and species-specific forward and reverse primers for *ECE1*) were used at a final concentration of 200 nM. qPCR amplifications were performed using a Rotor-gene system (Corbett). *ECE1* gene expression was calculated individually for each strain using the threshold cycle ($\Delta\Delta C_T$) method to calculate fold changes ($2^{\Delta\Delta CT}$) and using *ACT1* as the reference gene. Data were represented by comparing fold changes in expression after setting controls (YPD at time zero) to a value of 1.

Statistical analysis of data. Data sets of three or more were analyzed by one-way analysis of variance (ANOVA) with Tukey's *post hoc* comparison test using GraphPad Prism 9 software. Pairwise comparisons of data were analyzed using a two-tailed unpaired *t* test using GraphPad Prism 9 software. In all cases, a *P* value of $\leq$0.05 was taken to be significant.

SUPPLEMENTAL MATERIAL

Supplemental material is available online only.

FIG S1, TIF file, 0.1 MB.

ACKNOWLEDGMENTS

This work was supported by grants from The Wellcome Trust (214229_Z_18_Z), the Biotechnology & Biological Sciences Research Council (BB/N014677/1), the National Institutes of Health (DE022550), and the NIH Research at Guys and St. Thomas's NHS Foundation Trust and the King's College London Biomedical Research Centre (IS-BRC-1215-20006) to J.R.N. D.W. is supported by a Wellcome Trust senior research fellowship (214317/A/18/Z), the MRC, and the University of Exeter (MR/N006364/2). S.M. and B.H. are supported by The Wellcome Trust (215599/Z/19/Z). B.H. is also supported by German Research Foundation (Deutsche Forschungsgemeinschaft [DFG]) project number HU 528/20-1, Ece1-Peptides, and the Cluster of Excellence Balance of the Microverse under Germany's Excellence Strategy, EXC 2051, project identifier 390713860. C.D. received funding from the French Government's Investissement d'Avenir program (Laboratoire d'Excellence, Integrative Biology of Emerging Infectious Diseases, ANR-10-LABX-62-IBEID) and the Swiss National Science Foundation (grant CRSII5_173863). This research was funded in whole, or in part, by the Wellcome Trust (214229_Z_18_Z, 214317/A/18/Z, 215599/Z/19/Z). For the purpose of open access, the author has applied a CC BY public copyright license to any Author Accepted Manuscript version arising from this submission.

R.B., J.P.R., N.K., S.L., E.P., S.M., D.N.W., A.T., A.C.-G., and N.K.K. performed experimental work, and all authors analyzed data. J.P.R., J.R.N., C.D., C.M., D.L.M., D.W., B.H., J.H., N.O.P., and O.W.H. contributed to conceptual design. J.P.R. and J.R.N. wrote the draft manuscript. All authors contributed to critical evaluation and final editing of the manuscript prior to submission. J.R.N. supervised the project.

We declare no conflicts of interest.

REFERENCES

1. Dal Peraro M, van der Goot FG. 2016. Pore-forming toxins: ancient, but never really out of fashion. Nat Rev Microbiol 14:77–92. https://doi.org/10.1038/nrmicro.2015.3.
2. Los FCO, Randis TM, Aroian RV, Ratner AJ. 2013. Role of pore-forming toxins in bacterial infectious diseases. Microbiol Mol Biol Rev 77:173–207. https://doi.org/10.1128/MMBR.00052-12.
3. Moyes DL, Wilson D, Richardson JP, Mogavero S, Tang SX, Wernecke J, Hofs S, Gratacap RL, Robbins J, Runglall M, Murciano C, Blagojevic M, Thavaraj S, Forster TM, Hebecker B, Kasper L, Vizcay G, Iancu SI, Kichik N, Hader A, Kurzai O, Luo T, Kruger T, Kniemeyer O, Cota E, Bader O, Wheeler RT, Gutsmann T, Hube B, Naglik JR. 2016. Candidalysin is a fungal peptide toxin critical for mucosal infection. Nature 532:64–68. https://doi.org/10.1038/nature17625.
4. Nash AK, Auchtung TA, Wong MC, Smith DP, Gesell JR, Ross MC, Stewart CJ, Metcalf GA, Muzny DM, Gibbs RA, Ajami NJ, Petrosino JF. 2017. The gut mycobiome of the Human Microbiome Project healthy cohort. Microbiome 5:153. https://doi.org/10.1186/s40168-017-0373-4.
5. Brown GD, Denning DW, Gow NA, Levitz SM, Netea MG, White TC. 2012. Hidden killers: human fungal infections. Sci Transl Med 4:165rv13. https://doi.org/10.1126/scitranslmed.3004404.
6. Richardson JP, Mogavero S, Moyes DL, Blagojevic M, Kruger T, Verma AH, Coleman BM, De La Cruz Diaz J, Schulz D, Ponde NO, Carrano G, Kniemeyer O, Wilson D, Bader O, Enoiu SI, Ho J, Kichik N, Gaffen SL, Hube B, Naglik JR. 2018. Processing of *Candida albicans* Ece1p is critical for candidalysin maturation and fungal virulence. mBio 9:e02178-17. https://doi.org/10.1128/mBio.02178-17.
7. Liu J, Willems HME, Sansevere EA, Allert S, Barker KS, Lowes DJ, Dixson AC, Xu Z, Miao J, DeJarnette C, Tournu H, Palmer GE, Richardson JP, Barrera FN, Hube B, Naglik JR, Peters BM. 2021. A variant *ECE1* allele contributes to reduced pathogenicity of *Candida albicans* during vulvovaginal candidiasis. PLoS Pathog 17:e1009884. https://doi.org/10.1371/journal.ppat.1009884.
8. Richardson JP, Willems HME, Moyes DL, Shoaie S, Barker KS, Tan SL, Palmer GE, Hube B, Naglik JR, Peters BM. 2018. Candidalysin drives epithelial signaling, neutrophil recruitment, and immunopathology at the

vaginal mucosa. Infect Immun 86:e00645-17. https://doi.org/10.1128/IAI.00645-17.
9. Blagojevic M, Camilli G, Maxson M, Hube B, Moyes DL, Richardson JP, Naglik JR. 2021. Candidalysin triggers epithelial cellular stresses that induce necrotic death. Cell Microbiol 23:e13371. https://doi.org/10.1111/cmi.13371.
10. Allert S, Forster TM, Svensson CM, Richardson JP, Pawlik T, Hebecker B, Rudolphi S, Juraschitz M, Schaller M, Blagojevic M, Morschhauser J, Figge MT, Jacobsen ID, Naglik JR, Kasper L, Mogavero S, Hube B. 2018. *Candida albicans*-induced epithelial damage mediates translocation through intestinal barriers. mBio 9:e00915-18. https://doi.org/10.1128/mBio.00915-18.
11. Ho J, Yang X, Nikou SA, Kichik N, Donkin A, Ponde NO, Richardson JP, Gratacap RL, Archambault LS, Zwirner CP, Murciano C, Henley-Smith R, Thavaraj S, Tynan CJ, Gaffen SL, Hube B, Wheeler RT, Moyes DL, Naglik JR. 2019. Candidalysin activates innate epithelial immune responses via epidermal growth factor receptor. Nat Commun 10:2297. https://doi.org/10.1038/s41467-019-09915-2.
12. Verma AH, Zafar H, Ponde NO, Hepworth OW, Sihra D, Aggor FEY, Ainscough JS, Ho J, Richardson JP, Coleman BM, Hube B, Stacey M, McGeachy MJ, Naglik JR, Gaffen SL, Moyes DL. 2018. IL-36 and IL-1/IL-17 drive immunity to oral candidiasis via parallel mechanisms. J Immunol 201:627–634. https://doi.org/10.4049/jimmunol.1800515.
13. Moyes DL, Runglall M, Murciano C, Shen C, Nayar D, Thavaraj S, Kohli A, Islam A, Mora-Montes H, Challacombe SJ, Naglik JR. 2010. A biphasic innate immune MAPK response discriminates between the yeast and hyphal forms of *Candida albicans* in epithelial cells. Cell Host Microbe 8:225–235. https://doi.org/10.1016/j.chom.2010.08.002.
14. Verma AH, Richardson JP, Zhou C, Coleman BM, Moyes DL, Ho J, Huppler AR, Ramani K, McGeachy MJ, Mufazalov IA, Waisman A, Kane LP, Biswas PS, Hube B, Naglik JR, Gaffen SL. 2017. Oral epithelial cells orchestrate innate type 17 responses to *Candida albicans* through the virulence factor candidalysin. Sci Immunol 2:eaam8834. https://doi.org/10.1126/sciimmunol.aam8834.
15. Swidergall M, Khalaji M, Solis NV, Moyes DL, Drummond RA, Hube B, Lionakis MS, Murdoch C, Filler SG, Naglik JR. 2019. Candidalysin is required for neutrophil recruitment and virulence during systemic *Candida albicans* infection. J Infect Dis 220:1477–1488. https://doi.org/10.1093/infdis/jiz322.
16. Drummond RA, Swamydas M, Oikonomou V, Zhai B, Dambuza IM, Schaefer BC, Bohrer AC, Mayer-Barber KD, Lira SA, Iwakura Y, Filler SG, Brown GD, Hube B, Naglik JR, Hohl TM, Lionakis MS. 2019. CARD9(+) microglia promote antifungal immunity via IL-1beta- and CXCL1-mediated neutrophil recruitment. Nat Immunol 20:559–570. https://doi.org/10.1038/s41590-019-0377-2.
17. Kasper L, König A, Koenig P-A, Gresnigt MS, Westman J, Drummond RA, Lionakis MS, Groß O, Ruland J, Naglik JR, Hube B. 2018. The fungal peptide toxin candidalysin activates the NLRP3 inflammasome and causes cytolysis in mononuclear phagocytes. Nat Commun 9:4260. https://doi.org/10.1038/s41467-018-06607-1.
18. Rogiers O, Frising UC, Kucharikova S, Jabra-Rizk MA, van Loo G, Van Dijck P, Wullaert A. 2019. Candidalysin crucially contributes to Nlrp3 inflammasome activation by *Candida albicans* hyphae. mBio 10:e02221-18. https://doi.org/10.1128/mBio.02221-18.
19. Wu Y, Zeng Z, Guo Y, Song L, Weatherhead JE, Huang X, Zeng Y, Bimler L, Chang CY, Knight JM, Valladolid C, Sun H, Cruz MA, Hube B, Naglik JR, Luong AU, Kheradmand F, Corry DB. 2021. *Candida albicans* elicits protective allergic responses via platelet mediated T helper 2 and T helper 17 cell polarization. Immunity 54:2595–2610.e7. https://doi.org/10.1016/j.immuni.2021.08.009.
20. Schaller M, Mailhammer R, Grassl G, Sander CA, Hube B, Korting HC. 2002. Infection of human oral epithelia with *Candida* species induces cytokine expression correlated to the degree of virulence. J Invest Dermatol 118:652–657. https://doi.org/10.1046/j.1523-1747.2002.01699.x.
21. Jayatilake JA, Samaranayake LP, Lu Q, Jin LJ. 2007. IL-1alpha, IL-1ra and IL-8 are differentially induced by *Candida* in experimental oral candidiasis. Oral Dis 13:426–433. https://doi.org/10.1111/j.1601-0825.2007.01318.x.
22. Stokes C, Moran GP, Spiering MJ, Cole GT, Coleman DC, Sullivan DJ. 2007. Lower filamentation rates of *Candida dubliniensis* contribute to its lower virulence in comparison with *Candida albicans*. Fungal Genet Biol 44:920–931. https://doi.org/10.1016/j.fgb.2006.11.014.
23. Moyes DL, Murciano C, Runglall M, Kohli A, Islam A, Naglik JR. 2012. Activation of MAPK/c-Fos induced responses in oral epithelial cells is specific to *Candida albicans* and *Candida dubliniensis* hyphae. Med Microbiol Immunol 201:93–101. https://doi.org/10.1007/s00430-011-0209-y.
24. Willems HME, Lowes DJ, Barker KS, Palmer GE, Peters BM. 2018. Comparative analysis of the capacity of the *Candida* species to elicit vaginal immunopathology. Infect Immun 86:e00527-18. https://doi.org/10.1128/IAI.00527-18.
25. Silva S, Hooper SJ, Henriques M, Oliveira R, Azeredo J, Williams DW. 2011. The role of secreted aspartyl proteinases in *Candida tropicalis* invasion and damage of oral mucosa. Clin Microbiol Infect 17:264–272. https://doi.org/10.1111/j.1469-0691.2010.03248.x.
26. Moralez AT, Perini HF, Furlaneto-Maia L, Almeida RS, Panagio LA, Furlaneto MC. 2016. Phenotypic switching of *Candida tropicalis* is associated with cell damage in epithelial cells and virulence in *Galleria mellonella* model. Virulence 7:379–386. https://doi.org/10.1080/21505594.2016.1140297.
27. Yu S, Li W, Liu X, Che J, Wu Y, Lu J. 2016. Distinct expression levels of *ALS*, *LIP*, and *SAP* genes in *Candida tropicalis* with diverse virulent activities. Front Microbiol 7:1175. https://doi.org/10.3389/fmicb.2016.01175.
28. Huerta-Cepas J, Capella-Gutierrez S, Pryszcz LP, Marcet-Houben M, Gabaldon T. 2014. PhylomeDB v4: zooming into the plurality of evolutionary histories of a genome. Nucleic Acids Res 42:D897–D902. https://doi.org/10.1093/nar/gkt1177.
29. Sievers F, Wilm A, Dineen D, Gibson TJ, Karplus K, Li W, Lopez R, McWilliam H, Remmert M, Soding J, Thompson JD, Higgins DG. 2011. Fast, scalable generation of high-quality protein multiple sequence alignments using Clustal Omega. Mol Syst Biol 7:539. https://doi.org/10.1038/msb.2011.75.
30. Drozdetskiy A, Cole C, Procter J, Barton GJ. 2015. JPred4: a protein secondary structure prediction server. Nucleic Acids Res 43:W389–W394. https://doi.org/10.1093/nar/gkv332.
31. Rice P, Longden I, Bleasby A. 2000. EMBOSS: the European Molecular Biology Open Software Suite. Trends Genet 16:276–277. https://doi.org/10.1016/s0168-9525(00)02024-2.
32. Fernandez-Escamilla AM, Rousseau F, Schymkowitz J, Serrano L. 2004. Prediction of sequence-dependent and mutational effects on the aggregation of peptides and proteins. Nat Biotechnol 22:1302–1306. https://doi.org/10.1038/nbt1012.
33. Moyes DL, Murciano C, Runglall M, Islam A, Thavaraj S, Naglik JR. 2011. *Candida albicans* yeast and hyphae are discriminated by MAPK signaling in vaginal epithelial cells. PLoS One 6:e26580. https://doi.org/10.1371/journal.pone.0026580.
34. Murad AM, Lee PR, Broadbent ID, Barelle CJ, Brown AJ. 2000. CIp10, an efficient and convenient integrating vector for *Candida albicans*. Yeast 16:325–327. https://doi.org/10.1002/1097-0061(20000315)16:4<325::AID-YEA538>3.0.CO;2-#.
35. Rojko N, Dalla Serra M, Macek P, Anderluh G. 2016. Pore formation by actinoporins, cytolysins from sea anemones. Biochim Biophys Acta 1858:446–456. https://doi.org/10.1016/j.bbamem.2015.09.007.
36. Liu GL, Chi Z, Wang GY, Wang ZP, Li Y, Chi ZM. 2015. Yeast killer toxins, molecular mechanisms of their action and their applications. Crit Rev Biotechnol 35:222–234. https://doi.org/10.3109/07388551.2013.833582.
37. Peters BM, Shirtliff ME, Jabra-Rizk MA. 2010. Antimicrobial peptides: primeval molecules or future drugs? PLoS Pathog 6:e1001067. https://doi.org/10.1371/journal.ppat.1001067.
38. Rahman D, Mistry M, Thavaraj S, Challacombe SJ, Naglik JR. 2007. Murine model of concurrent oral and vaginal *Candida albicans* colonization to study epithelial host-pathogen interactions. Microbes Infect 9:615–622. https://doi.org/10.1016/j.micinf.2007.01.012.
39. Schonherr FA, Sparber F, Kirchner FR, Guiducci E, Trautwein-Weidner K, Gladiator A, Sertour N, Hetzel U, Le GTT, Pavelka N, d'Enfert C, Bougnoux M-E, Corti CF, LeibundGut-Landmann S. 2017. The intraspecies diversity of *C. albicans* triggers qualitatively and temporally distinct host responses that determine the balance between commensalism and pathogenicity. Mucosal Immunol 10:1335–1350. https://doi.org/10.1038/mi.2017.2.
40. Mogavero S, Sauer FM, Brunke S, Allert S, Schulz D, Wisgott S, Jablonowski N, Elshafee O, Kruger T, Kniemeyer O, Brakhage AA, Naglik JR, Dolk E, Hube B. 2021. Candidalysin delivery to the invasion pocket is critical for host epithelial damage induced by *Candida albicans*. Cell Microbiol 23:e13378. https://doi.org/10.1111/cmi.13378.
41. Walther A, Wendland J. 2003. An improved transformation protocol for the human fungal pathogen *Candida albicans*. Curr Genet 42:339–343. https://doi.org/10.1007/s00294-002-0349-0.
42. Rupniak HT, Rowlatt C, Lane EB, Steele JG, Trejdosiewicz LK, Laskiewicz B, Povey S, Hill BT. 1985. Characteristics of four new human cell lines derived from squamous cell carcinomas of the head and neck. J Natl Cancer Inst 75:621–635.